Nepal Journal of Science and Technology 12 (2011) 139-148

X–ray Photoelectron Spectroscopic Study on the Anodic Passivity of Sputterdeposited W–Ta Alloys in 12 M HCl

Jagadeesh Bhattarai
Central Department of Chemistry, Tribhuvan University, Kirtipur, Kathmandu
e-mail: bhattarai05@yahoo.com

Abstract

The role of a simultaneous additions of tungsten and tantalum on the anodic passivity of the passive films of the sputter–deposited nanocrystalline W–xTa alloys was studied using immersion tests, electrochemical measurements and X–ray photoelectron spectroscopic (XPS) analysis. The formation of spontaneous passive film on the alloys, which is composed of double oxyhydroxide of tungsten and tantalum ions are responsible for their higher corrosion resistance than those of the alloy–constituting elements in 12 M HCl solution open to air at 30°C. The quantitative surface analysis by XPS is clarified that the improved anodic passivity of the alloys than those of alloy–constituting elements is based on the formation of new anodic passive oxyhydroxide films composed of W^{6+} and Ta^{5+} ions. These films have higher protectiveness and stability than those of passive oxyhydroxide films of alloy–constituting elements, that is, oxyhydroxides of hexavalent tungsten and pentavalent tantalum after potentiostatic polarization for 1 h in 12 M HCl.

Key words: W–Ta alloys, sputter deposition, polarization curve, passivity, XPS surface analysis

Introduction

The formation of anodic passive films formed on the metals or alloys has gained great scientific interest for a long time. It is important from a practical point of view that the anodic film causes the passivity. The passivity of metals or alloys mostly concerns the corrosion resistance and hence the interest is focused on the chemical stability of the anodic passive films. On the other hand, the breakdown of the anodic passive films has been the subject of many investigations. The pitting corrosion is one of the most common and dangerous types of localized corrosion of the anodic films. Therefore, the immunity to pitting corrosion is one of the most interesting characteristics of the passivity of the metals or alloys.

The passivating elements such as tungsten and tantalum can improve corrosion resistance as well as the localized corrosion like pitting corrosion of alloys. The properties of the anodic passive films formed on tungsten metal had reported. Di Quarto *et al*. (1983) have been stated that the anodic film formed on tungsten showed a duplex structure consisting of an inner amorphous barrier–type anodic WO_3 film and outer porous crystalline layer. On the other hand, an insulating layer of WO_3 was formed by anodic polarization of tungsten in acidic environments (Johnson and Wu 1971). Several surface studies have been carried out for an understanding of the role of the tungsten in the passivation mechanisms of stainless steels in aggressive chloride media (Naka *et*

al. 1978; Bui *et al.* 1983; Wang and Merz 1984; Habazaki *et al.* 1991 a, 1991 b).

On the other hand, tantalum is widely known for its superior corrosion resistance in aggressive acidic media. Amorphous nickel–base alloys containing certain amounts of tantalum exhibit very high corrosion resistant in boiling acids (Kawashima *et al.* 1985). Lee *et al.* (1996, 1997) reported a beneficial effect of tantalum to improve the corrosion resistance of nickel–base alloys in 12 M HCl. A series of the sputterdeposited binary tantalum–containing alloys showed higher corrosion resistance than those of alloying elements due to spontaneous passivation in aggressive media (Shaw *et al.* 1991, Yoshioka *et al.* 1991, 1994, Kim *et al.* 1994, Park *et al.* 1996, Hashimoto *et al.* 1996, El–Moneim *et al.* 1997; Bhattarai *et al.* 1998 a).

It has been reported that the high corrosion resistance of the sputter–deposited binary and ternary tungsten–based alloys in 12 M HCl was based on the formation of new passive double oxyhydroxide films of tetravalent tungsten and alloy–constituting cations (Bhattarai 1998, 2010, 2011 a, 2011 b; Bhattarai *et al.* 1995, 1997, 1998 a, 1998 b, 1998 c). The tetravalent tungsten was the main oxidation state of tungsten for these tungsten–based binary alloys at +0.2 V (SCE) or lower potentials, while the hexavalent tungsten is the main oxidation state of tungsten at +0.4 V (SCE) or higher potentials in hydrochloric acid solutions. According to Habazaki *et al.* (1992), the passive film on tungsten was tetravalent tungsten oxyhydroxide and hexavalent tungsten oxyhydroxide was not the true passive film. However, the transpassivation of tungsten is clearly different from those of chromium and molybdenum. Transpassivation of chromium and molybdenum was resulted in sharp increases in the anodic current density in 12 M HCl solution (Kim *et al.* 1994, Park *et al.* 1996, Hashimoto 2007). By contrast, the present author has been reported in polarization curves of tungsten and tungsten–based binary alloys that the oxidation from the tetravalent state to the hexavalent state of tungsten did not lead to the transpassivation, although the anodic current density was significantly high. In this context, it is necessary and interesting to study the potential dependence of the surface composition of the anodic passive films formed on the sputter–deposited W–xTa alloys to clarify the mechanisms of the anodic passivity of the binary alloys in hydrochloric acids.

The main objectives of the present study are to characterize the surface composition and structure of the anodic passive films formed on the sputter–deposited binary W–xTa (x = 23 and 60 at%) alloys after potentiostatic polarization for 1 h in 12 M HCl solution open to air at 30°C using electrochemical measurements and X–ray photoelectron spectroscopic (XPS) analyses.

Methodology

The W–xTa (x = 23, 60 and 77 at%) alloys were prepared using direct current (DC) magnetron sputtering on glass substrate as described elsewhere (Bhattarai 1995, 1998). The structure of the sputter–deposited W–xTa alloys used in the present study was confirmed as nanocrystalline single phase solid solution from X–ray diffraction patterns having the apparent grain size ranges from 8–18 nm (Bhattarai 1998; Bhattarai *et al.* 1998 a).

Prior to immersion tests, electrochemical measurements and XPS analyses, the surfaces of the alloy specimens were mechanically polished with a silicon carbide paper up to grit number 1500 in cyclohexane, rinsed by acetone and dried in air. The average corrosion rate of the alloys was estimated from the weight loss after immersion for 168 h in 12 M HCl solution open to air at 30°C. Open circuit immersion and potentiostatic polarization at several potential values for 1 h in 12 M HCl solution were carried out. A platinum mesh and a saturated calomel electrode (SCE) were used as counter and reference electrodes, respectively. All the potentials given in this paper are relative to SCE.

Before and after open circuit immersion or potentiostatic polarization, composition of the surface films formed on the alloy specimens was analyzed using XPS (Shimadzu ESCA–850 photoelectron spectrometer). The XPS spectra over a wide binding energy region (0–1000 eV) were exhibited peaks of chlorine, carbon, oxygen, tungsten and tantalum. The integrated intensities of the C 1s, O 1s, W 4f and Ta 4f spectra were separately obtained for the quantitative surface analysis as described elsewhere (Bhattarai 1998). For the specimen polarized or immersed in 12 M HCl solution, the Cl 2p spectrum was detected at about 199 eV, which comes from chloride ions. However, the intensity of the Cl 2p peak was very low and hence the concentration of chloride ions was not considered in

the calculation. The binding energies of the electrons were calibrated using the method described elsewhere (Asami 1976; Asami and Hashimoto 1977). The peak binding energies of each peak were further corrected using the energy value of 285 eV for C 1s electron state. The composition and thickness of anodic passive films and the composition of the underlying alloy surface were quantitatively determined by a previously proposed method (Asami 1976) using integrated intensities of photoelectrons under the assumption of a three layer model of the outermost contaminant hydrocarbon layer of uniform thickness, the surface film of uniform thickness and the underlying alloy surface of X−ray photoelectron spectroscopically infinite thickness. The photoionization cross−section of the W 4f and Ta 4f electrons relative to the O 1s electrons used were 2.97 (Kawashima *et al.* 1984) and 2.617 (Kim *et al.* 1994), respectively.

Results and Discussion

Corrosion behavior and passivity of W−xTa alloys

The corrosion rates of the sputter−deposited W−Ta alloys and alloy−constituting elements were estimated from weight losses after immersion in 12 M HCl solution. The weight loss for each specimen was estimated two to three times and the average corrosion rate was calculated. Figure 1 shows the average corrosion rates of the W−23Ta, W−60Ta and W−77Ta alloys after immersion for 168 h in 12 M HCl solution at 30°C. The corrosion rates of the sputter−deposited tungsten and tantalum are also shown for comparison. The W−60Ta and W−77Ta alloys showed more than two orders of magnitude lower rate than that of sputter−deposited tungsten and even lower than that of sputter−deposited tantalum metal. However, the corrosion rate of the W−23Ta alloy shows almost same corrosion rate of the tantalum. This result clearly revealed that the corrosion resistance of the W−xTa alloys is surprisingly improved in 12 M HCl at 30°C. Consequently, it can be said that both tungsten and tantalum improve the corrosion resistance of the W−xTa alloys synergistically.

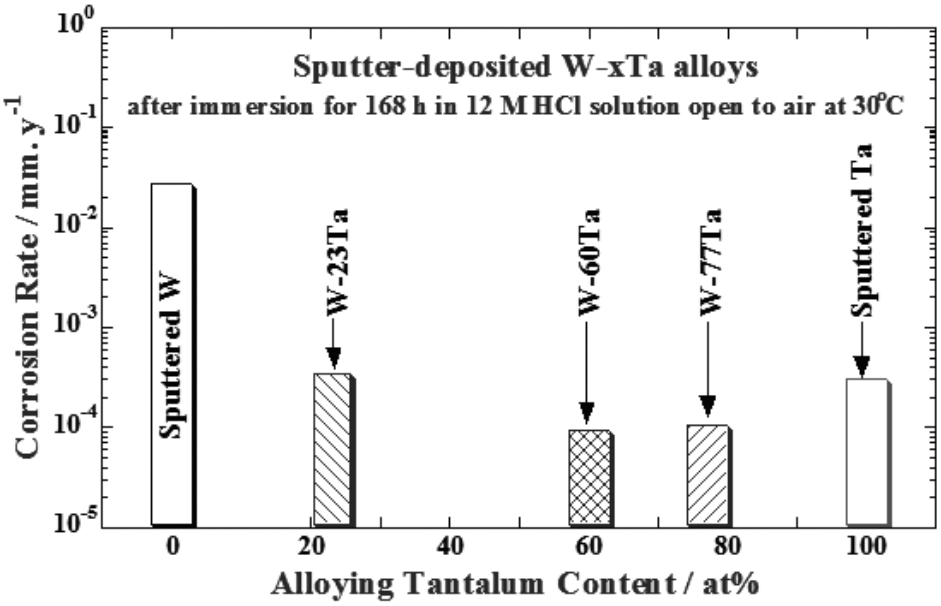

Fig.1. Corrosion rates of the sputter−deposited W−xTa alloys including tungsten and tantalum after immersion for 168 h in 12 M HCl solution open to air at 30°C.

Potentiostatic polarization measurements were carried out for the W–xTa alloys to gain a better understanding of the anodic passivity of the alloys after potentiostatic polarization for 1 h in 12 M HCl. Figure 2 shows the changes in anodic current densities of the W–23Ta and W–60Ta alloys as a function of polarization time. The anodic current densities of the alloys at all potentials are decreased with polarization time. According, the protective quality of the anodic passive films formed on the sputter–deposited W–xTa alloys increased with polarization time in 12 M HCl solution.

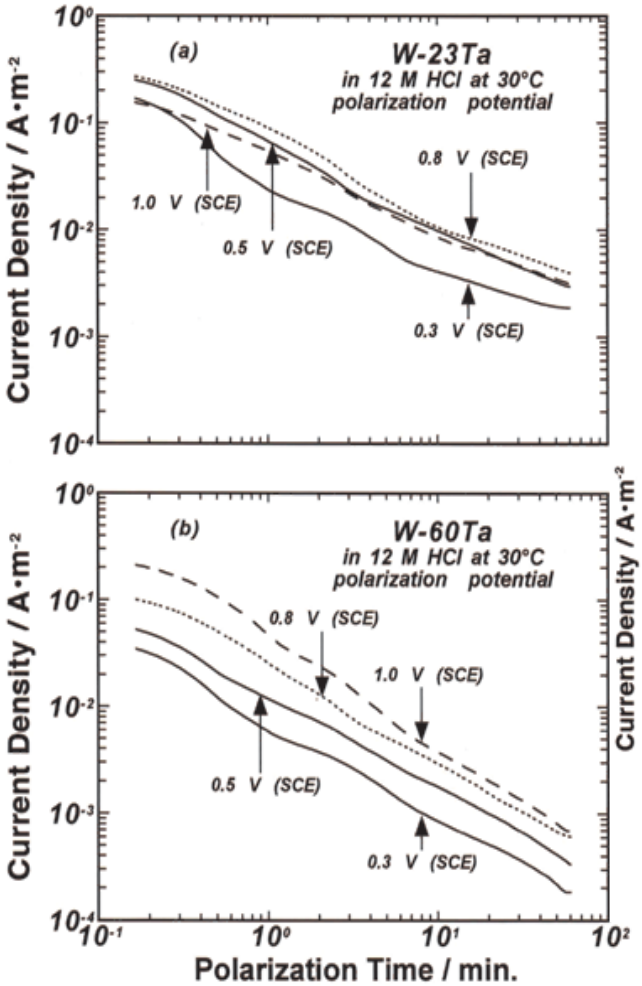

Fig.2. The change in the anodic current density with polarization time for the sputter–deposited (a) W–23Ta and (b) W–60Ta alloys after potentiostatic polarization for 1 h in 12 M HCl solution open to air at 30°C.

Figure 3 shows the potentiostatic anodic and cathodic polarization curves of the sputter–deposited W–23Ta and W–60Ta alloys including the sputter–deposited tantalum metal after potentiostatic polarization at different potentials for 1 h in 12 M HCl solution open to air at 30°C. Spontaneous passivation occurs for both the examined W–Ta alloys as well as tantalum metal. The open circuit potentials of the alloys are shifted to more positive direction than that of the sputter–deposited tantalum. The anodic current density of the alloys is decreased with increasing the tantalum content in the W–xTa alloys in 12 M HCl, indicating that the protectiveness of the anodic passive films formed on the W–Ta alloys is better than that of tungsten metal. Furthermore, it is meaningful to mention here that the W–60Ta alloy showed lowest anodic current density which is even lower that that of the sputter–deposited tantalum metal. Therefore, the W–xTa alloys containing adequate amount of tungsten showed the most stable passivity in the anodic potential region. These facts are in agreement with higher corrosion resistance than those of alloy–constituting elements as shown in Fig.1.

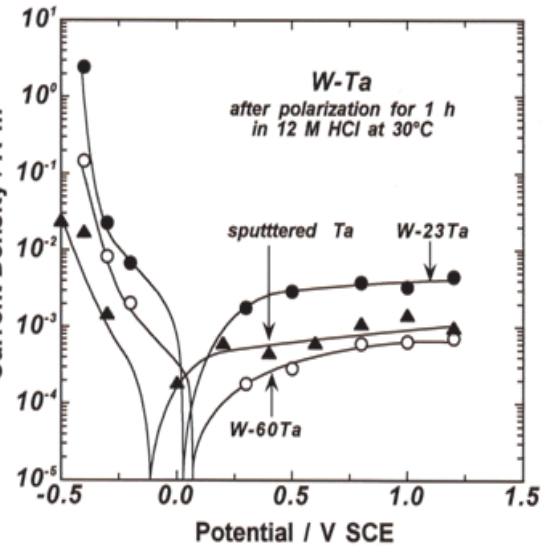

Fig.3. Potentiostatic cathodic and anodic polarization curves for the sputter–deposited W–23Ta, W–60Ta alloys including tantalum metal after potentiostatic polarization for 1 h in 12 M HCl solution open to air at 30°C.

Surface composition and passivity of W–xTa alloys

The surface analyses of the anodic passive films formed on the alloys give important information for a better understanding of the synergistic effect of tungsten and tantalum in the anodic passivity of the sputter–deposited W–xTa alloys. For this purpose, the surface of the W–xTa alloys before and after immersion or potentiostatic polarization for 1 h in 12 M HCl was analyzed immediately by XPS technique. XPS spectra for W–xTa alloys over a wide binding energy region, that is, 0–1000 eV, were exhibited peaks of tungsten, tantalum, oxygen, carbon and chlorine. The C 1s spectrum [Fig. 4 (a)] arose from a contaminant hydrocarbon layer covering the specimen surface was detected at about 285 eV. For the specimen polarized or immersed in 12 M HCl, the Cl 2p spectrum was detected at about 199 eV, which comes from chloride ions. The O 1s spectrum is composed of two peaks; the lower binding energy peak at 530.2–5331.1 eV is assigned to OM oxygen and the higher binding energy peak at 532.1–533.1 eV arises from OH oxygen (Asami 1976; Asami and Hashimoto 1977). The OM oxygen corresponds to O^{2-} ions in oxyhydroxide and/or oxide. The OH oxygen is linked to hydrogen and is composed of OH ions and bound water in the surface film. An example of an deconvolution of the O 1s spectrum measured for W–60Ta alloy is shown in Fig. 4 (b). The O^{2-} peak is substantially more intense than the OH peak in the O 1s spectrum measured for the alloy after immersion for 1 h in 12 M HCl. Accordingly, the passive films formed spontaneously on the alloy consist of oxyhydroxide in which O^{2-} ion is the major oxygen species.

The spectra from the alloy constituents indicated the presence of the oxidized and metallic species; the former comes from the surface film and the latter from the underlying alloy surface. The measured spectra of W 4f electrons and Ta 4f electrons were separated into W^{6+}, W^{5+}, W^{4+} and W^{m}, and Ta^{5+} and Ta^{m} state spectra, respectively. The superscripts, ″6+″, ″5+″, ″4+″and ″m″ denote hexavalent, pentavalent, tetravalent and metallic states, respectively. The most intense peaks of the W 4f and Ta 4f spectra are located very close to each other, and the Ta^{5+} $4f_{5/2}$ peak and the W^{m} $4f_{7/2}$ peak are superimposed as shown in Fig. 4 (c). On the other hand, the next intense peaks of the W 4d and Ta 4d electron spectra were completely overlapped each other. Therefore, the author used the W 4f and Ta 4f spectra for XPS analyses of the surface films formed on W–60Ta alloys. The standard spectra of tantalum metal, tungsten metal, pentavalent tantalum oxide and hexavalent tungsten oxide were used for the separation of metallic and oxidize states of all the measured Ta 4f and W 4f spectra, respectively. The shapes of W^{5+}

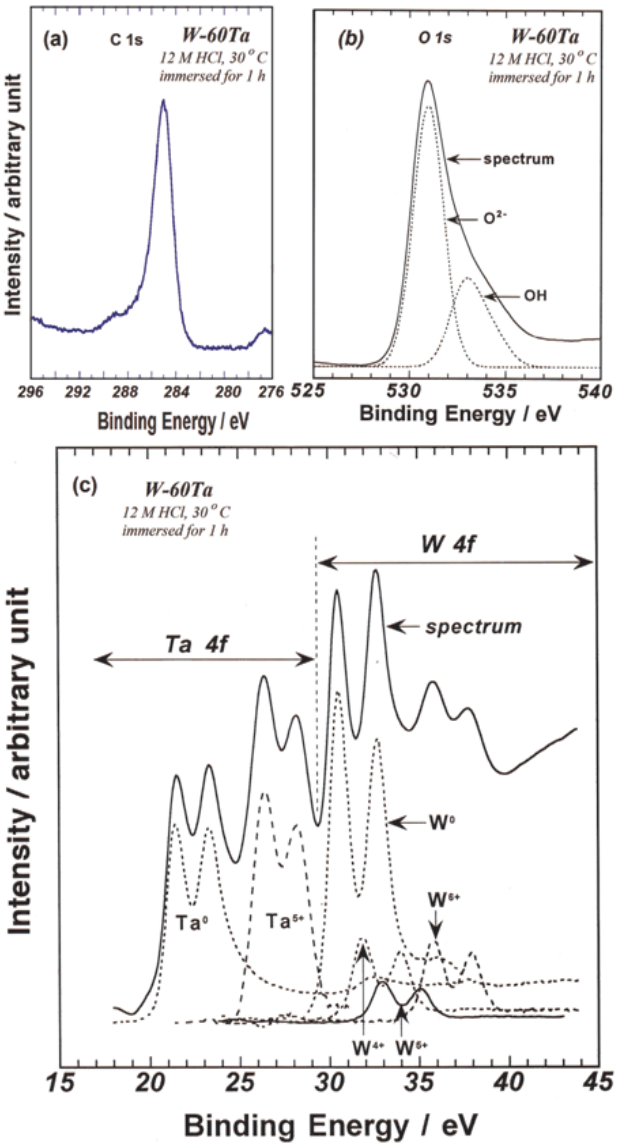

Fig.4. An example of (a) C 1s spectrum, (b) O 1s spectrum and (c) the deconvolution of W 4f and Ta 4f spectra measured for the sputter–deposited W–60Ta alloy after immersion for 1 h in 12 M HCl solution open to air at 30°C.

and W^{4+} 4f spectra were assumed to be same as the shape of the standard W^{6+} spectrum. Figure 4 (c) shows an example of the deconvolution of the W 4f spectrum as well as the Ta 4f spectrum measured for the W–60Ta alloy after immersion for 1 h in 12 M HCl at 30°C. Four doublets of the overlapped peaks can be identified in the W 4f spectrum, that is, three doublets of W^{6+}, W^{5+} and W^{4+} states and a pair of metallic state (W^m). The peaks appear at about 35.7 and 37.8, 32.9 and 35.0, 31.8 and 33.9, 30.4 and 32.5 eV, respectively. The integrated intensities of these W 4f spectra were separately obtained by the same method as that described elsewhere (Asami 1976, Asami and Hashimoto 1977). Similarly, a pair of metallic state peaks (Ta^m) at about 21.5 and 23.3eV, and a doublet of Ta^{5+} state peaks at about 26.3 and 28.1 eV can be identified in the Ta 4f spectrum for the W–60Ta alloy.

The changes in the surface compositions of the anodic films formed on the W–xTa alloys in 12 M HCl were analyzed by XPS. Figures 5 (a) and (b) show the changes in the cationic fractions in the surface films and the atomic fractions in the underlying alloy surface, respectively, as a function of the polarization potential. The cationic fractions in the air–formed films formed on as–polished specimens and atomic fractions in the underlying alloy surface of the as–polished specimens after mechanical polishing are also shown for comparison. Significant enrichment of tantalum in the passive films and the air–formed films with a consequent deficiency of the atomic fraction of tantalum in the underlying alloy surface is always seen. The cationic fraction of tantalum in the passive films is almost the same as the cationic composition of the air–formed film for the W–60Ta alloy, while the cationic composition of tantalum increases with potential for the W–23Ta alloy when the alloy is polarized in the transpassive potential region of tungsten [Fig. 5(a)]. On the other hand, the atomic fraction of tantalum is independent of the polarization potential in both W–23Ta and W–60Ta alloys as shown in Fig. 5(b), and is almost the same as the atomic fraction for the as–polished specimens.

As mentioned above in Fig. 4(b), the passive film formed spontaneously on the W–60Ta alloy consists of oxyhydroxides of both cations in which O^{2-} ion is a major oxygen species. Figures 6 (a) and (b) show the quantitative results of the ratios of $[OH^-]$/[cations] and $[O^{2-}]$/[cations] in the anodic passive films formed on the W–23Ta and W–60Ta alloys, respectively, as a function of the polarization potential. The ratio of $[O^{2-}]$/[cations] is increased with increasing anodic polarization potentials, while the ratio of $[OH^-]$/[cations] is slightly decreased with the polarization potential in the anodic direction. These results revealed that the anodic passive films formed on the W–23Ta and W–60Ta alloys are composed of oxyhydroxides of both tungsten and tantalum cations in which O^{2-} ions are remarkably higher than OH^- ions.

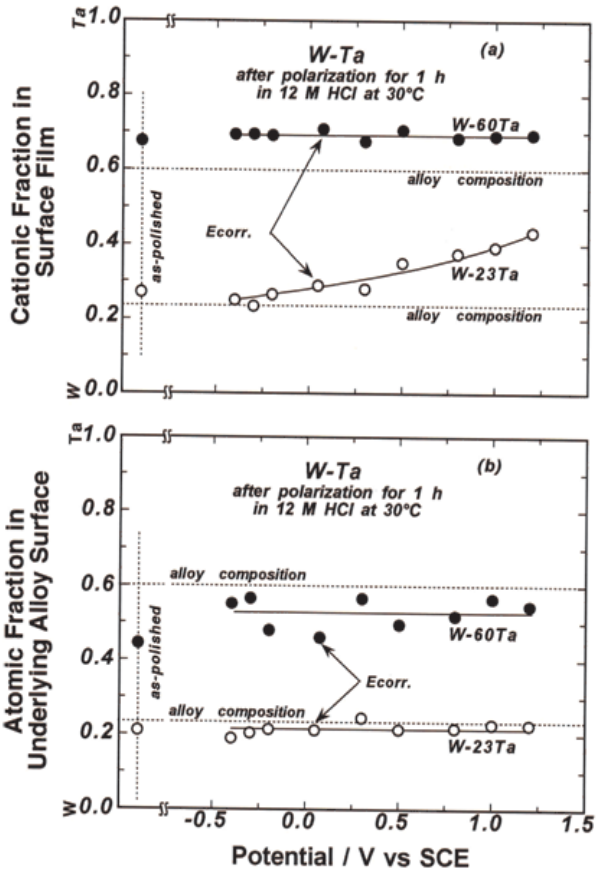

Fig.5. Changes in (a) cationic fractions in the surface films and (b) atomic fractions in the underlying alloy surface for the sputter–deposited W–23Ta and W–60Ta alloys after potentiostatic polarization for 1 h in 12 M HCl solution open to air at 30°C, as a function of polarization potential.

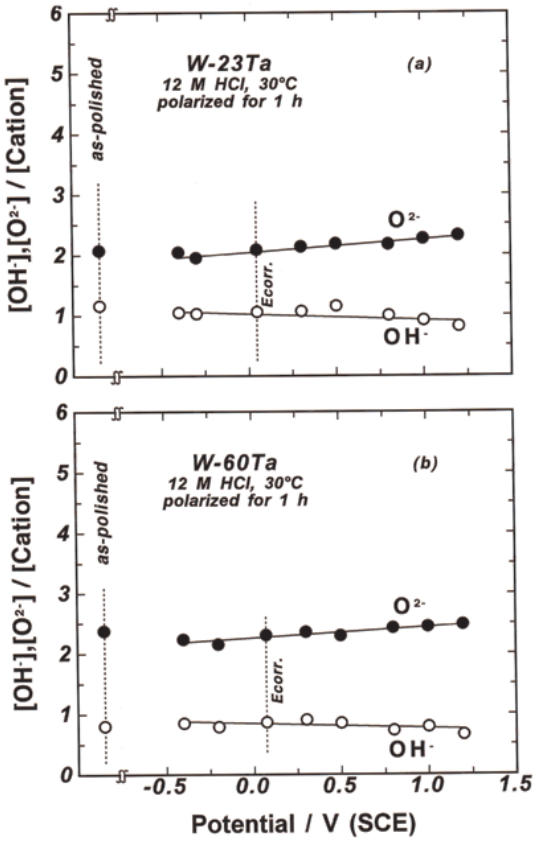

Fig.6. Changes in the ratios of $[O^{2-}]$/[cations] and $[OH^{-}]$/[cations] in the films formed on the sputter–deposited (a) W–23Ta and (b) W–60Ta alloys after potentiostatic polarization for 1 h in 12 M HCl solution open to air at 30°C, as a function of polarization potential.

Anodic film thickening and distribution of tungsten ions on W–xTa alloys

It has been reported that the anodic polarization leads to thickening of the anodic passive films for the sputter–deposited binary tungsten–based alloys in hydrochloric acid solutions (Bhattarai 1998). Remarkable anodic film thickening of the sputter–deposited tungsten–valve metal alloys was observed at +0.2 V (SCE) or higher potentials. The distribution of both cations of the binary tungsten–based alloys in the anodic passive films plays important roles in the film thickening of the alloys. Similarly, the change in different oxidation states of tungsten ions in the anodic film greatly affects the film thickening. Therefore, effects of cations of alloy–constituting elements, that is, tungsten ions and Ta^{5+} ions, in the anodic film thickening of the binary W–xTa alloys are discussed here in detail. Figure 7 shows the changes in the anodic film thickening of the W–xTa alloys after potentiostatic polarization for 1 h in 12 M HCl solution open to air at 30°C, as a function of potential. The anodic polarization on the W–xTa alloys including sputter–deposited tantalum leads to thickening of the anodic passive film. In particular, the anodic film thickening is clearly observed in the anodic potential range between 0.2 to 1.2 V (SCE).

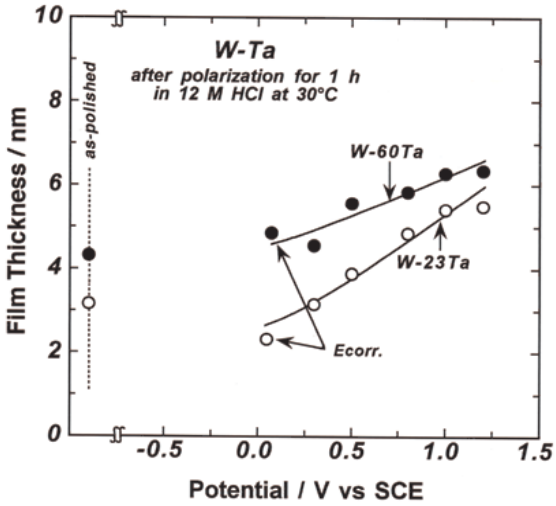

Fig.7. Changes in thicknesses of the anodic films formed on the sputter–deposited W–23Ta and W–60Ta alloys including tantalum metal after potentiostatic polarization for 1 h in 12 M HCl solution open to air at 30C, as a function of polarization potential.

The distribution of both cations of the binary W–xTa alloys, that is, W^{ox} and Ta^{5+} ions, in the anodic passivity of the alloys plays important roles in the film thickening of the alloys. Figures 8 (a) and (b) clearly show that the weights of both W^{ox} and Ta^{5+} ions are increased with anodic polarization, although the cationic fractions in the surface films is almost constant particularly for W–60Ta alloy as shown in Fig. 5. Similarly, the changes in different oxidation states of tungsten ion in the anodic film greatly affect the film thickening. Figure 9 (a) and (b) show the quantitative results of the change in the weights of W^{4+}, W^{5+} and W^{6+} ions in the films formed on W–23Ta and W–60Ta alloys, respectively. The W^{6+} ion increases with decreasing of W^{4+} and W^{5+} ions with anodic polarization for 1 h in 12 M HCl at 30°C. These results revealed that both cations of the W–Ta alloys contribute for the anodic film thickening. The main contribution among tungsten ions for the anodic film thickening of

the W–Ta alloys is W^{6+} ions, because a relatively stable and sparingly soluble W^{6+} ions increase remarkably in the anodic passive film in the potential region where film thickening is remarkable in 12 M HCl solution. Consequently, anodic polarization results in the anodic film thickening due to increase in W^{6+} and Ta^{5+} ions.

In conclusion, a beneficial effect of tungsten and tantalum in the passivity of the anodic passive films formed on the sputter–deposited binary W–xTa alloys is studied using electrochemical measurements and XPS analysis. The quantitative surface analyses by XPS are clarified that the improved anodic passivity of the alloys than those of alloy–constituting elements is based on the formation of new anodic passive oxyhydroxide films composed of W^{6+} and Ta^{5+} ions. These films have higher protectiveness and stability than those of passive oxyhydroxide films of alloy–constituting elements, that is, oxyhydroxides of hexavalent tungsten and pentavalent tantalum after potentiostatic polarization for 1 h in 12 M HCl solution open to air at 30°C.

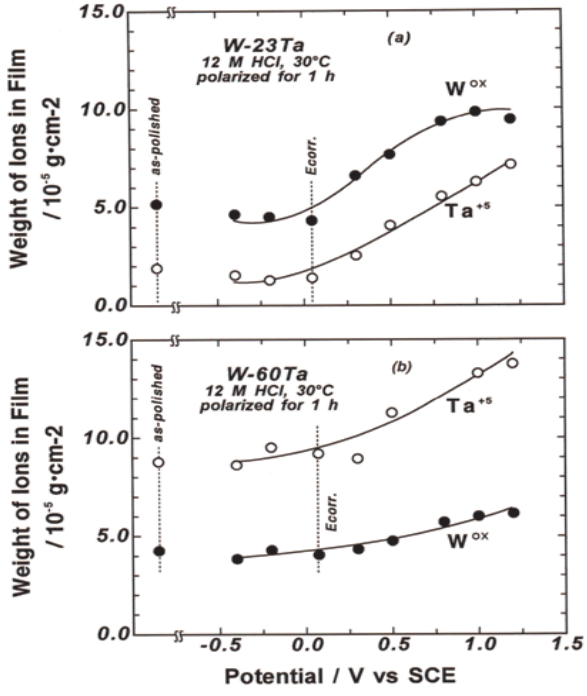

Fig.8. Changes in weights of cations in the surface films formed on the sputter–deposited (a) W–23Ta and (b) W–60Ta alloys after potentiostatic polarization for 1 h in 12 M HCl solution open to air at 30°C, as a function of polarization potential.

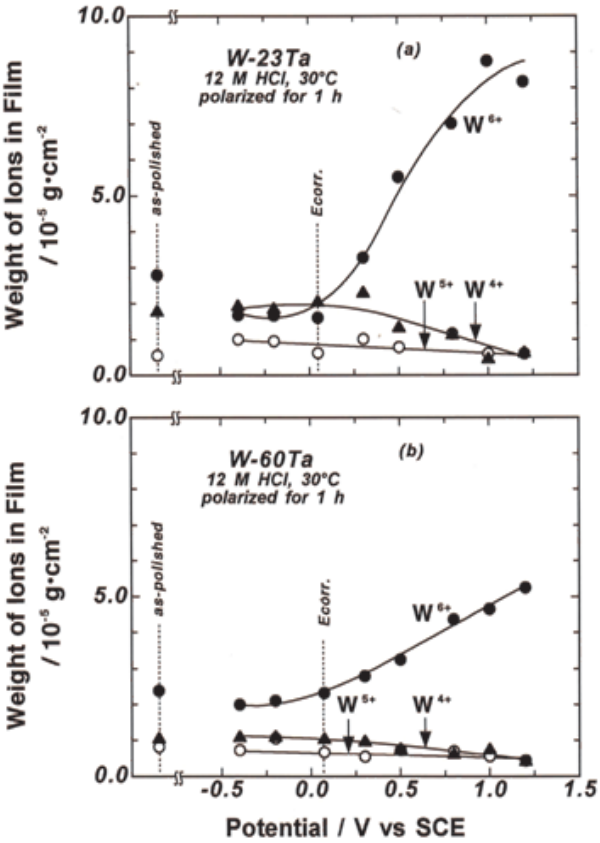

Fig.9. Changes in weights of W^{4+}, W^{5+} and W^{6+} ions in the surface films formed on the sputter–deposited (a) W–23Ta and (b) W–60Ta alloys after potentiostatic polarization for 1 h in 12 M HCl solution open to air at 30°C, as a function of polarization potential.

Acknowledgements

Author would like to express his sincere gratitude to Professor Emeritus; Dr. K. Hashimoto, Dr. K. Asami and Dr. A. Kawashima of IMR of Tohoku University, Sendai and Professor Dr. H. Habazaki of Hokkaido University for their kind help and discussions on the XPS analysis. Author is thankful to Japan Government and Diaki Ataka Engineering Co. Ltd. for providing an opportunity to visit Tohoku Institute of Technology, Japan as a Research Fellow.

References

Asami, K. 1976. A precisely consistent energy calibration method for X–ray photoelectron spectroscopy. *Journal of Electron Spectroscopy and Related Phenomena* **9:**469–478.

Asami, K. and K. Hashimoto. 1977. The X−ray photoelectron spectra of several oxides of iron and chromium. *Corrosion Science* **17:**559"570.

Bhattarai, J. 1995. *Corrosion behavior of sputter-deposited tungsten-base alloys.* Research Reports, Institute for Materials Research (IMR), Tohoku University, Sendai, Japan, 43+IV pp.

Bhattarai, J. 1998. *Tailoring of corrosion resistance tungsten alloys by sputtering.* Ph. D. thesis, Department of Materials Science, Tohoku University, Japan. 229 pp.

Bhattarai, J. 2010. X−ray photoelectron spectroscopic analyses on the corrosion−resistant W−Cr−Ni alloys in 12 M HCl. *Transactions of the Materials Research Society of Japan* **35 (1):**1−6.

Bhattarai, J. 2011 a. The corrosion behavior of sputter−deposited ternary W−Zr−(1518)Cr alloys in 12 M HCl. *African Journal of Pure and Applied Chemistry* **5 (8):**212−218.

Bhattarai, J. 2011 b. X−ray photoelectron spectroscopic study on the anodic passivity of sputter−deposited W−Nb alloys 12 M HCl solution. *Journal of Scientific Research* **3(3):**457"470.

Bhattarai, J., E. Akiyama, A. Kawashima, K. Asami and K. Hashimoto. 1995. The corrosion behavior of sputter−deposited amorphous W−Ti alloys in 6 M HCl solution. *Corrosion Science* **37:**2071"2086.

Bhattarai, J., E. Akiyama, H. Habazaki, A. Kawashima, K. Asami and K. Hashimoto. 1997. Electrochemical and XPS studies of the corrosion behavior of sputter−deposited amorphous W−Zr alloys in 6 and 12 M HCl solutions. *Corrosion Science* **39:**355−375.

Bhattarai, J., E. Akiyama, H. Habazaki, A. Kawashima, K. Asami and K. Hashimoto. 1998 a. The passivation behavior of sputter−deposited amorphous W−Ta alloys in 12 M HCl solution. *Corrosion Science* **40:**757−779.

Bhattarai, J., E. Akiyama, H. Habazaki, A. Kawashima, K. Asami and K. Hashimoto. 1998 b. Electrochemical and XPS studies of the corrosion behavior of sputter−deposited amorphous W−Nb alloys in concentrated hydrochloric acid solutions. *Corrosion Science* **40:**19"42.

Bhattarai, J., E. Akiyama, H. Habazaki, A. Kawashima, K. Asami and K. Hashimoto. 1998 c. Electrochemical and XPS studies of the passivation behavior of sputter" deposited W−Cr alloys in 12 M HCl solution. *Corrosion Science* **40:**155−175.

Bui, N., A. Irhzo, F. Dabosi, Y. Limouzin−Maire. 1983. On the mechanism of improved passivation by addition of tungsten to austenitic stainless steels. *Corrosion* **39:**491−496.

Di Quarto, F., S. Piazza and C. Sunseri. 1983. Passivity of Metals and Semiconductors. *Proceedings of 5th International Symposium on Passivity* (ed. M. Froment). The Societe de Chimie Physique, Bombanners, France. 497 pp.

El−Moneim, A. A., E. Akiyama, H. Habazaki, A. Kawashima, K. Asami and K. Hashimoto. 1997. The corrosion behavior of sputter−deposited amorphous Mn−Ta alloys in 0.5 M NaCl solution. *Corrosion Science* **39:**1965−1979.

Habazaki, H., A. Kawashima, K. Asami and K. Hashimoto. 1991 a. *in Proceeding of the Symposium on the Application of Surface Analysis Methods to Environment/ Material Interactions* (eds. D. R. Baer, C. R. Clayton and G. D. Davis).The Electrochemical Society, Inc., Pennington, USA. 467 pp.

Habazaki, H., A. Kawashima, K. Asami and K. Hashimoto. 1991 b. The effect of tungsten on the corrosion behavior of amorphous Fe−Cr−W−P−C alloys in 1 M HCl. *Journal of Electrochemical Society* **138:**76−81.

Habazaki, H., A. Kawashima, K. Asami and K. Hashimoto. 1992. The corrosion behavior of amorphous Fe−Cr−Mo−P−C and Fe−Cr−W−P−C alloys in 6 M HCl solution . *Corrosion Science* **33:**225−232.

Hashimoto, K. 1993. Chemical properties of rapidly solidified alloys. in *Rapidly Solidified Alloys; Processes, Structures, Properties, Applications* (ed. Howard H. Liebermann), Marcel Dekker Inc., New York. pp. 591−615.

Hashimoto, K. 2007. The role of corrosion−resistant alloying elements in passivity. *Corrosion Science* **49:** 42−52.

Hashimoto, K., H. Habazaki, E. Akiyama, H. Yoshioka, J. H. Kim, P. Y. Park, A. Kawashima and K. Asami. 1996. Recent progress in corrosionresistant new alloys prepared by sputter deposition. *The Science Reports of the Research Institutes Tohoku University* **A42:**99−105.

Johnson, J. W. and C. L. Wu. 1971. *Journal of Electrochemical Society* **118:**1909.

Kawashima, A., K. Shimamura, S. Chiba, T. Masunaga, K. Asami and K. Hashimoto. 1985. in *Proc. 4th Asian−Pacific Corrosion Control Conference, Tokyo*. **Vol. 2:**1042 pp.

Kawashima, A., K. Asami and K. Hashimoto. 1994. *Corrosion Science* **24:**807−812.

Kim, J. H., E. Akiyama, H. Habazaki, A. Kawashima, K. Asami and K. Hashimoto. 1994. An XPS study of the corrosion behavior of sputter−deposited amorphous Cr−Nb and Cr−Ta alloys in 12 M HCl solution. *Corrosion Science* **36:**511−523.

Lee, H.−J., E. Akiyama, H. Habazaki, A. Kawashima, K. Asami and K. Hashimoto. 1996. The corrosion behavior of amorphous and crystalline Ni−10Ta−20P alloys in 12 M HCl. *Corrosion Science* **38:**1269−1279.

Lee, H.−J., E. Akiyama, H. Habazaki, A. Kawashima, K. Asami and K. Hashimoto. 1997. The roles of tantalum and phosphorus in the corrosion behavior of Ni−Ta−P alloys in 12 M HCl. *Corrosion Science* **39:**321−332.

Naka, M., K. Hashimoto and T. Masumoto. 1978. High corrosion resistance of amorphous Fe–Mo and FeW alloys in HCl. *Journal of Non–Crystalline Solids* **29:**61–65.

Park, P.Y., E. Akiyama, A. Kawashima, K. Asami and K. Hashimoto. 1996. The corrosion behavior of sputter–deposited Mo–Ta alloys in 12 M HCl solution. *Corrosion Science* **38:** 397–411.

Shaw, B. A., T. L. Fritz, G. D. Davis and W. C. Moshier. 1991. The influence of tungsten additions on the passivity of aluminum. *Journal of Electrochemical Society* **138:**3288–3295.

Wang, R. and M. D. Merz. 1984. Corrosion resistance of amorphous FeNiCrW alloys. *Corrosion Science* **40:**272–280.

Yoshioka, H., A. Kawashima, K. Asami and K. Hashimoto. 1991. An XPS study of the corrosion behavior of sputter–deposited amorphous Al–W alloys in 1 M HCl. *Corrosion Science* **32:**313–325.

Yoshioka, H., H. Habazaki, A. Kawashima, K. Asami and K. Hashimoto. 1993. Corrosion, Electrochemistry and Catalysis of Metastable Metals and Intermetallics (eds C. R. Clayton and K. Hashimoto). The Electrochemical Society, 72 pp.